Retrieving Cirrus Vertical Cross Sections of Extinction, Effective Particle Size, and Ice-Water Content with GOES Imager Data

Robert P. d'Entremont and Gary B. Gustafson
Satellite Meteorology Group
Atmospheric and Environmental Research, Inc., Lexington, MA

David L. Mitchell
Atmospheric Sciences Division
Desert Research Institute, Reno NV

Abstract: Global information of ice water content (IWC) in ice clouds is urgently needed for testing of global climate models (GCMs) and other applications, but satellite and ground-based retrievals of IWC and the column-integrated IWP are still in the developing stages, and tend to have large uncertainties (as high as a factor of 2 or more, depending on the radiance data used). A retrieval method is presented here that may have relatively low uncertainties, using one or more thermal channels routinely available on operational meteorological and environmental satellites.

Recent research indicates that ice cloud radiative properties depend on more than effective diameter (D_{EFF}) and ice water content (IWC). The size distribution shape, or dispersion, such as the degree of bimodality, is also an important factor at thermal wavelengths. Failure to account for this can lead to substantial retrieval errors. Hence, we have developed a retrieval scheme that accounts for the size distribution (SD) shape in mid-latitude and tropical cirrus.

For a given ice-particle shape, preliminary tests varying particle size, IWC and cloud depth, as well as accounting for surface emission and instrument noise, suggest the scheme is accurate to about ±15% over an IWP range of 1 to 100 g m^{-2}, and about ±25% over an IWP range of 100 to 200 g m^{-2}, except for very thin cirrus having unusually large crystals or multiple cloud layers. This is based on thousands of radiation transfer model retrieval simulations.

With an integrated IWP retrieval in hand, we couple it with cloud-top and cloud-base retrievals and inferences on normalized IWC-profile shapes to infer vertical profiles of cirrus radiative and microphysical properties such as the extinction coefficient and (an absolute-magnitude) IWC profile. The retrieval scheme is being tested with satellite-based retrievals and compared against in-situ radar and lidar data and from over two dozen cirrus IOPs between January and December 2005 that occurred over Hanscom AFB near Boston, Massachusetts. GOES-8 channels at 6.5 and 10.7 μm were used.

1 Introduction

Our project has three main goals: (1) develop and refine space-based retrieval methods for cirrus top, base, and ice-water path (IWP); (2) infer ice-water content (IWC), effective ice-particle size (D_{EFF}), and visible extinction optical thickness (OT) profiles using thermal infrared data from the 6.7 and 11-μm wavelength bands available on GOES; and (3) compare these retrievals with coincident ground-based lidar and radar observations taken over Hanscom AFB. We are only required to retrieve cloud properties for optically thinner cirrus; when cirrus is optically thick (with TIR emissivities on the order of 0.3 or higher), all that is required is a flag denoting their presence.

Our approach has three main steps: (1) identify cirrus pixels in GOES imager data using multispectral infrared cloud-detection tests (d'Entremont and Gustafson, 2003); (2) estimate cirrus base, top, and IWP; and (3) from these estimates infer the IWC and particle-size profiles, which in turn are used to diagnose extinction coefficient profiles.

Traditional satellite-based retrievals of IWP are still in the developing stages inasmuch as they can have large uncertainties depending on the type of cirrus size-distribution and ice-particle shape assumed. A deterministic analysis of our retrieval method is presented here that may have relatively low uncertainties under certain viewing conditions, using several thermal-radiance channels. Those conditions are described here along with a mathematically based estimate of expected IWP retrieval accuracies.

Recent research indicates that ice-cloud infrared radiative properties are not always uniquely specified by effective diameter (D_{EFF}) and ice water content (IWC). The size distribution shape, or dispersion, and the degree of bimodality also play an important role at thermal wavelengths (Mitchell, 2002). On the other hand, based on new information on ice particle mass- and area-dimensional relationships, ice particle shape uncertainties now appear to have minimal adverse influence on our cirrus IWP retrievals (Andy Heymsfield, personal communication). This is because new data show that the geometric cross-section of the ice-particle distributions is similar for bullet rosettes and planar polycrystals, two ice-particle types most commonly observed in cirrus clouds (Korolev et al., 2000). However, this does not preclude having to account for all possible sizes, especially small sizes, in the distribution of cirrus ice particles.

Consequently, our retrieval scheme accounts for a bimodal size-distribution (SD) shape in mid-latitude and tropical cirrus (see Mitchell et al., 2000; Ivanova et al., 2000; Ivanova et al., 2004). We use a bimodal shape for what are termed the small (particles

with long-axis diameter D < 100 μm) and large modes (D > 100 μm) of the SD. Here the term "effective diameter" D_{EFF} is meant as the ratio of the third to second moments of the SD. Using a channel centered near 6.7 μm (the water-vapor (WV) band), absorption is a cross-sectional-area dominated radiative process, dependent on the SD and ice-particle shape. At the 12-μm thermal infrared (TIR) the same is true, although generally absorption is stronger here than in the water-vapor band (the imaginary refractive index is higher). In mid-latitudes, model simulations that bracket the natural range of SD variations suggest that our WV-TIR IWP retrieval scheme is accurate to ±15% over an IWP range of 0 to 80 g m^{-2}, and to about ±25% over an IWP range of 80 to 100 g m^{-2} for the coldest cirrus clouds. These accuracies correspond to retrieved 6.7-μm emissivities of ~0.95, along with errors in cirrus temperature that span the natural range of expected values. This is illustrated by the plot on the left side of Figure 1. The plot on the right is for tropical cirrus. In the tropics, WV-TIR IWP retrievals are reliable only out to 50 g m^{-2} or so for very cold cirrus (because the presence of many small particles, with sizes on the order of 10 μm or less, dominate the absorption process), corresponding to cirrus visible extinction optical thicknesses between 3 and 10 (depending more precisely on particle shape and size). The IWP retrieval range extends well beyond 100 g m^{-2} for warmer cirrus, where optical thicknesses reach 10 and higher.

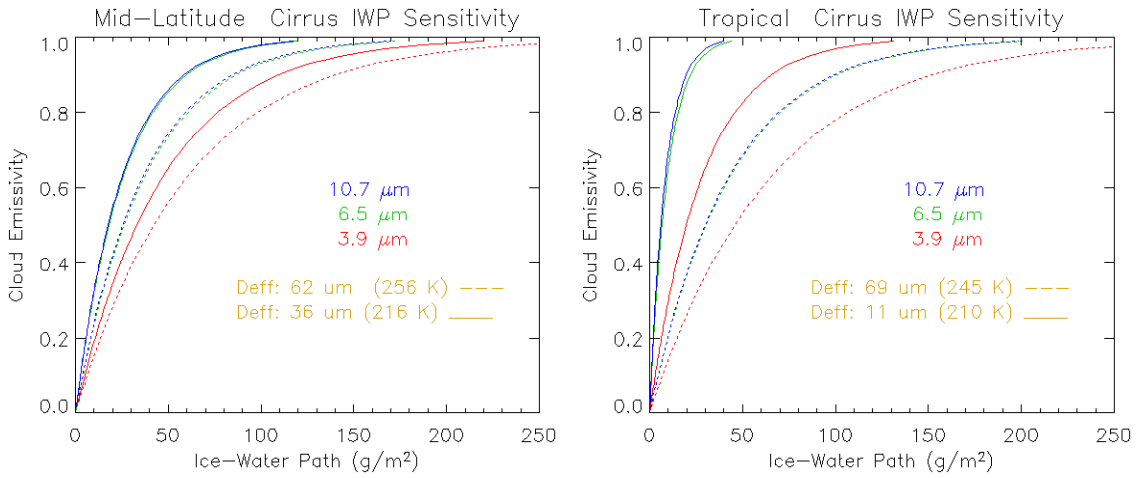

Figure 1. Plots of cirrus IWP as a function of emissivity for mid-latiutude and tropical cirrus size distributions, as prescribed by the SDs of Ivanova et al. (2000).

Because the MWIR imaginary refractive index for ice is quite small (MWIR ~ 0.005, WV ~ 0.05, TIR ~ 0.3), ice-particle cross-sections play a smaller role in governing electromagnetic energy exchange. In the MWIR, absorption is largely an ice-volume-dependent radiative process. This is a handy property to exploit since it reduces IWP retrieval uncertainties due to particle shape, which more strongly govern area-

dependent absorption. Radiation-transfer model simulations in mid-latitudes that vary particle size, IWC and cloud depth suggest our IWP retrieval scheme is accurate to about ±15% over an IWP range of 1 to 100 g m^{-2}, and about ±25% over an IWP range of 100 to 200 g m^{-2}, except for very thin cirrus having unusually large crystals or multiple cloud layers. In the tropics the corresponding accuracy ranges are reduced to 110 and 150 g m^{-2}, respectively, which map to cirrus visible extinction optical thicknesses 5 and higher.

There are two clear choices for cirrus retrievals: WV-TIR and MWIR-TIR. Each has one major advantage and one disadvantage for our particular application. The range of the MWIR-TIR IWP retrieval space is 0-150 g m^{-2}, indicating that MWIR bands offer good sensitivity to cirrus ice-mass estimates, important for accurate extinction calculations. However, in the daytime, MWIR radiances contain an emitted thermal and a reflected solar component. Since our technique is based on emitted infrared energy, the reflected solar component must be removed from the MWIR cirrus observations before attempting to retrieve cirrus properties. This requires a priori knowledge of attributes such as particle size, optical thickness, and even particle shape since 3.9-µm cirrus reflectances depend on these properties. If these were known properties then there would be no need for real-time cirrus retrievals. Obviously reflected sunlight is a non-issue at night, raising the possibility for generating cirrus products with MWIR-TIR data whenever the sun is below the horizon. This has the advantage of increasing the sensitivity of our satellite-based techniques to large IWPs.

Similarly, WV-TIR retrievals have advantages and shortcomings. In mid-latitudes the range of IWP retrieval space is only 0-100 g m^{-2}, but WV radiances are dominated both day and night by cirrus emission processes. Recall that for our application simple detecting the presence of optically thick cirrus (with emissivities greater than 0.3 or so) is all that is required of our algorithm; thus for cirrus transmittance applications it is important only to retrieve microphysical and radiative properties where clouds with lower IWPs exist. For clouds with higher IWPs a quantitative estimate of extinction is not required since the cloud is so optically thick and the transmittance so small. Additionally, continuity of cirrus retrievals is maintained across the terminator transition zone. For these reasons we have chosen to use WV-TIR retrieval algorithms, although we have discussed theoretically the use of MWIR data should a decision be made to use them in the future.

We have also made computational improvements to our algorithms over the past year, most notably with an increase in speed of two orders of magnitude in the cirrus processing portions of our codes: from 10^{-3} sec to 10^{-5} sec per cirrus pixel, on average.

2 Notation

$B_\lambda(T)$ Planck blackbody monochromatic radiance, W m^{-2} μm^{-1} $ster^{-1}$
$B_N(T)$ Planck blackbody equivalent monochromatic radiance for satellite sensor band "N," W m^{-2} μm^{-1} $ster^{-1}$
D_{EFF} Ice-particle effective diameter, μm
ε Effective emissivity, dimensionless
I_N Band-weighted upwelling infrared radiance, W m^{-2} μm^{-1} $ster^{-1}$
λ Wavelength, μm
M, N Sensor channel designations
Q_{ABS} Absorption efficiency factor, dimensionless ratio of radiative and physical cross sections
$R_N(\lambda)$ Response function for band "N," dimensionless
T Temperature, K
τ Optical thickness, dimensionless
t Transmittance, dimensionless
z Height, m

3 Cirrus Infrared Radiative Transfer Model

The observed upwelling radiance $I_{OBS,N}$ in satellite channel "N" for an infinitesimally thin cirrus slab is expressed in terms of the cirrus bulk emissivity ε_{CI} as

$$(1) \qquad I_{OBS,N} = (1 - \varepsilon_{CI,N}) I_{CLR,N} + \varepsilon_{CI,N} B_N (T_{CI}) t_{ATM} ,$$

where "t_{ATM}" is the atmospheric transmittance between cirrus top and TOA. It is typically prescribed using radiative transfer codes and NWP water-vapor and temperature soundings. Conditions under which (1) must be used are discussed in later sections. For now, we shall assume that cirrus radiance observations from two window channels are available.

3.1 Formulating the Retrieval Problem

The quantities ε_{CI} and T_{CI} in Eq. (1) are descriptors of the spatial, radiative, and microphysical properties of a cirrus cloud. Exploiting a cloud mask (see d'Entremont and Gustafson, 2003) to identify nearby cirrus-free radiances provides an estimate for $I_{CLR,N}$, leaving two unknowns in emissivity and effective temperature. With only one equation the solution is mathematically ill-posed; it is necessary to add at least one more equation to the problem. Writing (1) for two wavelength window bands "N" and "M" yields

(2a) $$I_{OBS,N} = (1 - \varepsilon_{CI,N}) I_{CLR,N} + \varepsilon_{CI,N} B_N (T_{CI}) t_{ATM,N}$$

and

(2b) $$I_{OBS,M} = (1 - \varepsilon_{CI,M}) I_{CLR,M} + \varepsilon_{CI,M} B_M (T_{CI}) t_{ATM,M} ,$$

which at the outset appears to be a well-posed set of two equations in two unknowns ε_{CI} and T_{CI}. However the cirrus emissivity $\varepsilon_{CI,X}$ is a wavelength-variant quantity with dependences on the imaginary refractive index at wavelength λ_X, as well as on ice-particle size and shape, and the bimodal size distribution N(D). Thus in introducing a second equation we have also introduced a new unknown in $\varepsilon_{CI,M}$. It is therefore necessary to relate $\varepsilon_{CI,M}$ to the other "original" unknowns $\varepsilon_{CI,N}$ and/or T_{CI}. This need motivates the development of an absorption theory for non-spherical ice crystals that is outlined next.

3.2 Modeling Cirrus Microphysics

A deterministic relationship among cirrus emissivities at multiple wavelengths, effective particle size, and temperature is described here. Each is addressed individually in the following sections, and then combined into one cohesive theory useful for solving Eqs. (2a) and (2b) simultaneously.

Effective diameter (D_{EFF}) and the anomalous diffraction theory of van de Hulst (1981) turn out to be important concepts in our modeling approach, and they relate our retrieved quantities with other variables of interest, such as cirrus ice water content (IWC) and ice-water path (IWP).

3.2.1 Ice-Particle Effective Diameter

We define effective diameter D_{EFF} with respect to irregularly shaped ice crystals as the ratio of the third and second moments of the size distribution N(D), where D is the long-axis dimension of an ice particle. Conceptually its meaning can be understood using the concept of effective distance or photon path, d_E. This is the particle volume-to-area ratio as first suggested by Bryant and Latimer (1969), and further developed in Mitchell (200x) to treat absorption and extinction by ice particles. In these studies d_E is defined as the particle volume V at bulk ice density divided by the particle's projected area P at random orientation:

(3) $$d_E = m / (\rho_{ICE} P) ,$$

where m is the particle's mass, and bulk ice density ρ_{ICE} = 0.92 g cm^{-3}. This value of ρ_{ICE} must be used since the ice refractive indices we use in our model are referenced to bulk ice density. This concept of d_E is borne out of the anomalous diffraction approximation (ADA), a simplification of Mie theory (van de Hulst, 1981). Absorption processes represented in ADA are based on the principle of effective photon path, indicating that d_E is the relevant dimension for autonomous particle-radiation interactions.

We can take this one step further and relate the diameter of a sphere, D, to its effective distance, d_E. Using ice spheres as an example in (3), mass m = ρ_{ICE} (π $D^3/6$) and projected area P = π $D^2/4$, giving

$$d_E = 2/3\ D\ . \tag{4}$$

If there is an effective photon path for a single particle, it can be asked if there is also an effective photon path D_E for the collection of ice particles that comprise the cirrus. The gamma size distribution is used to describe the number of cirrus ice particles with effective diameter D:

$$N(D) = N_o\ D^v\ e^{-\Lambda D}\ , \tag{5}$$

with dispersion and slope parameters v and Λ, respectively. Based on the formalism used in Eq. (3) but extended to the entire distribution of ice particles,

$$D_E = IWC\ /\ (\ \rho_{ICE}\ P_{TOT}\ )\ , \tag{6}$$

where IWC is the cirrus ice-water content (ice mass per unit volume), and where P_{TOT} is the total projected area of all ice particles in the size distribution (with units of area per unit volume; e.g., $cm^2\ cm^{-3} = cm^{-1}$). In other words, projected area P_{TOT} is the geometric cross-sectional area per unit volume of a distribution (5) of ice particles with random orientations. Based on Eq. (4), the effective diameter of the size distribution should then be 3/2 d_E or

$$D_{EFF} = 3\ IWC\ /\ (\ 2\ \rho_{ICE}\ P_{TOT}\ )\ . \tag{7}$$

Mitchell (2002) continues on from this point to show that there is one general definition for effective diameter, $\int D^3\ N(D)\ dD\ /\ \int D^2\ N(D)\ dD$, for all clouds regardless of phase, and that this definition can be understood physically as the representative photon path for the collection of particles in the size distribution. In the next section the relationship between cirrus absorption efficiency and effective diameter is

described.

3.2.2 Absorption of Infrared Radiation by Ice Clouds

ADA approximates the absorption efficiency $Q_{ABS,ADA}$ for a single ice particle as

$$Q_{ABS,ADA} = 1 - \exp(-4\pi n_I d_E / \lambda) ,$$

where n_I is the imaginary part of the refractive index at wavelength λ. As defined in Eq. (4), d_E is the representative distance a photon travels through a particle without internal reflections or refraction occurring. Substituting Eq. (4) for $d_E = 2/3\ D_{EFF}$ into the above expression yields

(8) $$Q_{ABS,ADA} = 1 - \exp(-8\pi n_I D_{EFF} / 3\lambda) ,$$

where $Q_{ABS,ADA}$ is now the geometric-optics absorption efficiency representing the entire size distribution based on ADA and the concept of effective photon path.

This expression describes mathematically the absorption due only to a size distribution's geometric cross section. Mitchell (200y) shows that relevant particle-radiation interaction processes not included in ADA can be parameterized in terms of ADA such that this modified ADA yields absorption efficiencies with errors ~10% or less relative to Mie theory. Namely, Eq. (8) has been expanded by Mitchell (200y) to include the processes of internal reflection/refraction and photon "tunneling," which collectively are well approximated by

(9) $$Q_{ABS} = (1 + C_1 + C_2) Q_{ABS,ADA} .$$

The leading term (the "1") on the right side of Eq. (9) represents absorption via the particle's cross section; the term C_1 accounts for absorption due to internal reflection and refraction; and C_2 is the "photon tunneling" term. Tunneling here is a process by which photons beyond the particle's geometric cross-section are absorbed. For spheres, Mie theory prescribes the "tunneling factor" as 1; for irregularly shaped ice particles, this factor lies between 0 and 1. The term denoted as "C_2" above contains dependences on this tunneling factor. See Appendix A for a more detailed discussion of tunneling.

Expressions for the constants C_1 and C_2 are given in Mitchell (200y) and are not repeated here, except to note that they depend on ice-crystal particle size, shape, wavelength, and index of refraction.

The coefficient for absorption by a randomly oriented ice particle is defined as

$$\beta_{ABS} = \int_0^\infty Q_{ABS}(D,\lambda)\, P(D)\, N(D)\, dD \,, \tag{10}$$

where Q_{ABS} is the absorption efficiency at wavelength λ for ice crystals of effective diameter D, P(D) is the projected area for a crystal of dimension D, and N(D) is the ice-crystal particle size distribution as given by Eq. (5). If D_{EFF} is the appropriate dimension for describing particle-radiation interactions for an entire size distribution, then it is natural to ask what the consequences might be if the absorption efficiency Q_{ABS} were to be taken outside the integral of (10), and expressed in terms of D_{EFF}. This results in the following simple equation

$$\beta_{ABS} = \overline{Q}_{ABS}\, P_{TOT} \,, \tag{11}$$

where $\overline{Q}_{ABS}$ is the absorption efficiency representing the entire size distribution; and where

$$P_{TOT} = \int_0^\infty P(D)\, N(D)\, dD \tag{12}$$

is the geometric cross-section area of the entirety of randomly oriented ice particles in the cirrus cloud, with units of area per unit volume (e.g., $cm^2\ cm^{-3} = cm^{-1}$). For irregularly shaped crystals it is easy to comprehend that P(D) is a function of crystal shape and size. Using the projected-area dimensional power law expression $P = \sigma D^{\delta}$ (see Mitchell, 1996; 200z) for an individual ice crystal of a given shape, and substituting Eq. (5) for N(D) into Eq. (12) yields

$$P_{TOT} = \int_0^\infty \sigma N_o D^{\delta+v} e^{-\Lambda D}\, dD \,. \tag{13}$$

This in turn can be integrated analytically to yield

$$P_{TOT} = \sigma N_o \Gamma(\delta+v+1) \;/\; \Lambda^{\delta+v+1} \,. \tag{14}$$

Solving Eq. (11) for absorption efficiency finally yields

(15) $$\overline{Q}_{ABS} = \beta_{ABS} / P_{TOT} .$$

Both the absorption coefficient β_{ABS} and the cross-sectional area P_{TOT} of the entire size distribution N(D) are dependent on both amount and shape of the ice particles that comprise the cirrus cloud. However, the absorption efficiency $\overline{Q}_{ABS}$ is a normalized metric of absorption that depends only on crystal size, shape, wavelength, and refractive index.

Mitchell (200x) has derived an analytic expression for β_{ABS} for a "representative" unit volume of actual ice-crystal size distributions, with explicit dependences

(16) $$\beta_{ABS} = \beta_{ABS} (\sigma, \delta, \nu, \Lambda)$$

on the area power-law and size-distribution parameters σ, δ, ν, and Λ. A detailed analysis of Eq. (16) is not repeated here (see Mitchell, 200x) except to note with importance that the absorption coefficient β_{ABS} is dependent on the shape of the size distribution N(D) as prescribed by the dispersion and slope parameters ν and Λ, respectively; and on ice-crystal shape as well via the projected-area power-law coefficients σ and δ. Recall now the introductory remarks concerning cross-sectional area and ice-particle shape. Although not detailed here, Eq. (16) offers physical and mathematical insight into the importance of these wavelength-independent properties.

With a means available for computing β_{ABS} and P_{TOT}, their ratio yields a distribution's absorption efficiency $\overline{Q}_{ABS}$ for the entire SD as prescribed by Eq. (15). Such computations have been performed and compared with numerical Mie theory integrations over size distributions of water droplets, and against observations of absorption efficiencies for non-spherical ice crystals (see Mitchell, 200w); Figure A1 in Appendix A shows the comparison results. Errors relative to $\overline{Q}_{ABS,MIE}$ are low (generally within 10%), and for small ice crystals grown in a cloud chamber the errors between observation, T-matrix calculations, and the modified ADA theory are within 3% at wavelengths between 2 and 18 μm (Mitchell, 200w). With an approach in hand for computing absorption efficiency, a basis is established for computing cirrus infrared emissivities in our retrieval paradigm, which is outlined next.

3.2.3 Cirrus Emissivity

One of the major output components of our retrieval approach [as defined by simultaneous solution of Eqs. (2a) and (2b)] is the estimated emissivity ε at the thermal infrared reference wavelength 11 μm. Assuming no scattering at the WV and TIR

wavelengths,

(17) $$\varepsilon = 1 - \exp(-\tau_{ABS} / \cos\theta_{SAT}) ,$$

where θ_{SAT} is the satellite zenith angle and τ_{abs} is the absorption optical depth. Dividing optical depth by the factor $\cos\theta_{SAT}$ adjusts the path length through the cirrus due to non-nadir views. For an infinitesimally thin cirrus cloud where the size distribution (SD) is invariant with in-cloud position, the absorption optical depth is given by

(18) $$\tau_{ABS} = \beta_{ABS} \Delta z ,$$

where Δz is the cloud physical depth (from base to top) and β_{ABS} is the absorption coefficient, represented here by Eq. (16) and fully defined in Mitchell (200x). The assumption of an invariant size distribution is consistent with our idealized cirrus thin-slab assumption (recall Eq. (1)), but it brings with it potential errors that are discussed further along in the applications sections.

3.2.4 Ice Water Path

Equation (7) can now be exploited to solve for the ice water path IWP, which is the melted-equivalent water mass per unit area of a vertical column through the entire extent of the cirrus cloud. By definition, and assuming that IWC is the vertically averaged value,

$$IWP = IWC \ \Delta z$$

and Eq. (7) becomes

(19) $$D_{EFF} = 3 \ IWP / (2 \ \rho_{ICE} \ P_{TOT} \ \Delta z) .$$

Solving for β_{ABS} in Eqs. (11) and (18) and equating the two expressions gives

$$P_{TOT} = \tau_{ABS} / (\overline{Q}_{ABS} \ \Delta z) .$$

Inserting this result into (19) for P_{TOT} and solving for ice-water path,

(20) $$IWP = 2 \ \rho_{ICE} \ D_{EFF} \ \tau_{ABS} / (3 \ \overline{Q}_{ABS}) .$$

Substituting (20) for τ_{ABS} in (17), the cirrus emissivity is expressed as

(21) $$\varepsilon = 1 - \exp[\, -3\, IWP \cdot \overline{Q}_{ABS} / (2\, \rho_{ICE}\, D_{EFF} \cos\theta_{SAT})\,].$$

Solving Eq. (21) for IWP yields

(22) $$IWP = -2\, \rho_{ICE}\, D_{EFF} \cos\theta_{SAT} \ln(1 - \varepsilon) / (3 \cdot \overline{Q}_{ABS}) .$$

Note that D_{EFF} appears both in the numerator and in the denominator, since $\overline{Q}_{ABS}$ is dependent on particle size effective diameter via Eq. (8).

3.2.5 Visible Extinction Optical Thickness

The extinction coefficient (absorption plus scattering) is defined mathematically as

$$\beta_{EXT} = \int_0^\infty Q_{EXT}(D,\lambda)\, P(D)\, N(D)\, dD .$$

At visible solar wavelengths ($\lambda \approx 0.5$ μm) it is well known that the extinction efficiency $Q_{EXT,VIS}$ is accurately approximated as 2 for ice particles in cirrus. This corresponds to size parameters $\pi D / \lambda \geq 30$. At and near wavelengths of 0.5 μm, size parameters greater than 30 correspond to size-distribution effective diameters $D_{EFF} > 5$ μm. Ice particles as observed in natural cirrus always satisfy this condition, even at the tropical tropopause. With $Q_{EXT,VIS} = 2$ and using the definition for P_{TOT} in (12), the above expression for visible extinction coefficient can be written

$$\beta_{EXT,VIS} = 2\, P_{TOT} .$$

Solving Eq. (7) for P_{TOT} and noting that the extinction optical thickness $\tau_{EXT,VIS} = \beta_{EXT,VIS}\, \Delta z$, we have finally that

(23) $$\tau_{EXT,VIS} = 3\, IWP / (\rho_{ICE}\, D_{EFF}) .$$

3.2.6 Numerical Considerations

With an expression now in hand to compute emissivity at any wavelength, as prescribed by (21), let's re-examine the original problem of two equations in three unknowns $\varepsilon_{ci,m}$, $\varepsilon_{ci,n}$, and T_{ci}. In Eq. (21) it is seen that several new unknowns have been introduced to the set of equations, including D_{EFF}, IWP, and the coefficients σ, δ,

v, and Λ. Instead of helping to bring the number of equations and unknowns into line, it seems that there are now even more unknowns (the aforementioned six plus T_{CI}) than equations [three: (2a), (2b), and (21)].

Fortunately, we have exploited a means of estimating the size distribution parameters v and Λ, and consequently D_{EFF}, in tropical anvil and mid-latitude cirrus as a function of cirrus environmental temperature (Mitchell et al., 2000; Ivanova et al., 2000, 2004). The tropical scheme is based on 93 size distributions from three tropical anvils reported in McFarquhar and Heymsfield (1997) for the CEPEX field campaign, three tropical anvils reported in Knollenburg et al. (1993), and a tropical tropopause cirrus case (Heymsfield, 1984). The mid-latitude scheme is based on over 1000 in-situ measurements of cirrus taken during ARM and FIRE campaigns in the central U.S. (Ivanova et al., 2000). Exploiting this parameterization means that D_{EFF} and the SD dispersion and slope coefficients v and Λ are all explicit functions of temperature T_{CI} only. Notationally,

(24a) $$D_{EFF} = D_{EFF}(T_{CI}) ,$$

(24b) $$v = v(T_{CI}) ,$$

and

(24c) $$\Lambda = \Lambda(T_{CI})$$

as prescribed by Ivanova et al. (2000). The projected-area power-law coefficients σ and δ are functions of an assumed particle shape as tabulated by Mitchell (2002) [we usually pick planar polycrystals or bullet rosettes, cited as most common in nature by the recent literature (Korolev, 2000)]. If at some future time it is found that ice particle shape is strongly dependent on cirrus environmental temperature, this easily can be incorporated into our retrieval algorithm. Fortunately, in the meantime, the difference in geometric and radiative properties between polycrystals and rosettes is small (Andy Heymsfield, personal communication).

Exploiting these relationships reduces the number of equations/unknowns to 3/4, seemingly leaving only ice water path as the "extra" variable. However the numerical approach to solving the three simultaneous equations is fundamentally one of repeatedly guessing at the set { $\varepsilon_{CI,N}$, $\varepsilon_{CI,M}$, T_{CI} } until it satisfies simultaneously the set of equations. Thus all we need is a way to obtain $\varepsilon_{CI,M}$ *given* a guess value $\varepsilon_{CI,N}$. Writing Eq.(24) for two wavelengths λ_N and λ_M and setting the wavelength-invariant "IWP = IWP" results in

$$-2\,\rho_{ICE}\,D_{EFF}\cos\theta_{SAT}\ln(1-\varepsilon_{CI,N}) / (3\,\overline{Q}_{ABS,N}) \;=\; -2\,\rho_{ICE}\,D_{EFF}\cos\theta_{SAT}\ln(1-\varepsilon_{CI,M}) / (3\,\overline{Q}_{ABS,M})\ .$$

All the wavelength-independent quantities cancel during simplification leaving

(25a) $$\varepsilon_{CI,M} \;=\; 1-(1-\varepsilon_{CI,N})^{R}\ ,$$

where the absorption-efficiency-ratio exponent R is defined as

(25b) $$R \;=\; \overline{Q}_{ABS,M} / \overline{Q}_{ABS,N}\ .$$

Since the absorption efficiencies $\overline{Q}_{ABS}$ are dependent on effective particle size [see Eq. (19)], the N(D) dispersion, and its slope [recall Eqs. (14) and (16)], and since each of these is a function only of the cirrus temperature [via Eq. (24)], then $\overline{Q}_{abs}$ is expressible as a function of T_{CI} as well, along with the ratio R:

(26) $$\overline{Q}_{ABS}(D_{EFF},\lambda) \;\doteq\; \overline{Q}_{ABS}\left[\,D_{EFF}(T_{CI}),\,\lambda\,\right] \;\equiv\; \overline{Q}_{ABS}(T_{CI},\,\lambda)\ .$$

We have finally reduced the mathematical problem to one of three equations [(13a), (13b), and (25)] in three unknowns $\varepsilon_{CI,N}$, $\varepsilon_{CI,M}$, and T_{CI}. Cirrus IWP is thus a diagnostic, derived product of the retrieval, e.g., once the emissivity is found it can be used with Eq. (22) to retrieve ice water path, or vice versa via Eq. (21).

The numerical recipe of our cirrus retrieval algorithm is reviewed here. Given imager radiance data with two thermal infrared window bands centered on wavelengths λ_N and λ_M, along with a pre-computed pixel-level cloud mask that identifies all cirrus clouds, then:

(a) Use the cloud mask (d'Entremont and Gustafson, 2003) to compute nearby averages of the cirrus-free radiances $I_{CLR,N}$ and $I_{CLR,M}$ for each cirrus pixel, based on the background geography type;

(b) Guess at the set { IWP, T_{CI} } of cirrus ice-water path and temperature. Use T_{CI} to determine D_{EFF}, v, Λ, $Q_{ABS}(D_{EFF}, \lambda_N) \doteq \overline{Q}_{ABS,N}$, and $\overline{Q}_{ABS,M}$ as described in this section, and compute $\varepsilon_{CI,N}$ as prescribed by Eq. (21);

(c) Using (25), compute the ratio R and the value of $\varepsilon_{CI,M}$ that is physically consistent

with with $\varepsilon_{CI,N}$; and

(d) Check to see whether the guess set { IWP, T_{CI} } of cirrus attributes satisfies Eqs. (2a) and (2b) simultaneously for the satellite radiance observations $I_{OBS,N}$ and $I_{OBS,M}$ in bands "N" and "M" for the cirrus pixel in question. If so, stop. If not, re-iterate starting at Step (b).

The question of how to iterate on a guess is an important one if computational timeliness is an issue. Binary search techniques or "brute-force" methods that consider all mathematically plausible combinations of { IWP, T_{CI} } are two possible strategies. We use a hybrid of these two options and retrieve cirrus properties at speeds of 10^{-5} sec per pixel on a PC with a Linux OS.

Figure 2 illustrates graphically the process of retrieving cirrus ice-water path and effective temperature. Plotted for the WV and TIR infrared bands are all mathematically possible pairs of IWP and T_{ci} for a given set of satellite radiance observations. The radiance observations correspond to a 6.5-μm WV brightness temperature of 227.8 K, and a 10.7-μm TIR temperature of 247.5 K. Note that for a single sensor band the number of theoretically possible pairs (IWP,T_{ci}) is infinite. This ambiguity is resolved, however, by choosing the pair that satisfies the satellite upwelling radiance equations simultaneously at the two infrared wavelengths. This is the fundamental basis of our retrieval paradigm.

4 Estimates of Cirrus Top and Base

With a method now in place for determining cirrus effective temperature and, by way of NWP RAOBs, the cirrus effective height, the next step is to estimate cirrus top and base. Our retrievals of cloud top and cloud base are based on pixel-level retrievals of the emissivity-adjusted effective cloud temperature T_{CI} in Eq. (2). Eventually this temperature is converted to altitude using satellite-coincident NWP upper-air forecasts of temperature, pressure, and geopotential.

Once the pixel-level effective temperatures are computed, we exploit the "local" texture of the effective-temperature retrievals to estimate cloud top and cloud base. For cloud vertical boundaries we look at the effective temperatures of pixels "near" the edges of a cloud mass. By "near" is meant "those pixels that lie within a prescribed, tunable radius of the analysis pixel." Currently this radius is set in our production runs (see www.aer.com/cloud) by default to ten 4-km GOES infrared pixels for both cloud base and cloud top. A frequency distribution of these temperatures is assembled for all pixels within the tunable radius, and the base-temperature (top-temperature) estimates

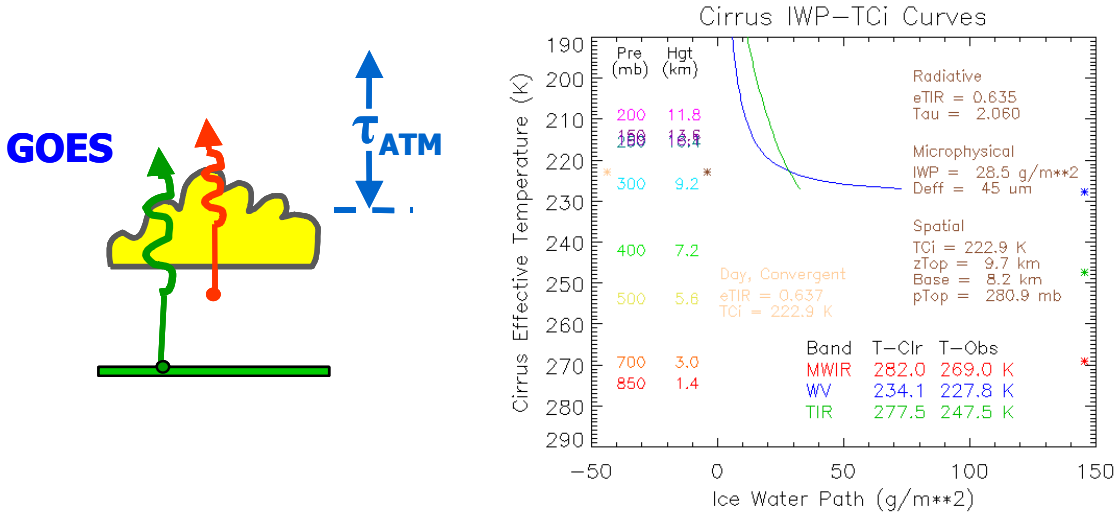

Figure 2. Graphical depiction of the retrieval method outlined in Section 3.2.6. The curve crossing point denotes the cirrus IWP and temperature retrieval for this pixel.

are assigned as the mean of the temperatures that fall above (below) the median effective temperature of the local histogram.

Horizontal irregularities in satellite-derived effective temperature retrievals are based on lots of small-magnitude influences: sensor noise, an incorrect estimate of the cloud-free radiance (I_{CLR} in Eq. (2)), and inaccurate NWP T-z soundings name a few. Nonetheless we exploit the spatial structure of the "raw" pixel-level effective temperature retrievals to infer cloud top (usually within a very localized region) and cloud base (within a more "regional" region), for both water-droplet and ice-particle clouds. At the moment we use no information from the NWP upper-air profiles other than to convert the base and top temperatures to height. Although empirically based, we observe some diagnostic skill in this texture-based approach, as is illustrated next.

4.1 GOES Cirrus Retrievals and Ground-Based Lidar/Radar Observations

As mentioned in the introductory sections, satellite and ground-based cirrus observations for more than two dozen case days were collected over Hanscom AFB near Boston, MA during 2005, including vertically pointing ground based radar and lidar along with radiosondes and environmental satellites. The data collection periods have been event driven, based on the presence of at least one cirrus cloud layer visible to the eye over the Hanscom site. Because of the emphasis on cirrus transmittance, the basic go/no-go criteria for any given day was "the presence of at least one broken or overcast cirrus layer, in the absence of scattered low and middle clouds." The cloud

cover should be of at least three hours duration, to allow at least ½ hour of AFCPR (Air Force Cloud Profiling Radar) 35-GHz radar and PEELS (Portable Eye-Safe Environment Lidar System) 1.574-μm lidar operation before a radiosonde launch and 2½ hours after. Each declared observing day has at least one 3-hour observing period.

To the date of this writing (Nov 05) 27 days have met measurement criteria and at least three-hours of observations were collected each day. We have used this unique data set to evaluate the performance of our cirrus extinction and IWC-profile retrieval algorithm using coincident GOES-12 cirrus analyses. During the measurement periods, GOES-12 (GOES East) satellite data are analyzed using the technique outlined in Sections 3 and 4.1 to retrieve the set of cirrus bulk properties listed in Table 1, at the GOES infrared pixel level (with a nominal 4-km spatial resolution at satellite subpoint).

- Cloud mask, cloud phase (ice or water)
- Effective temperature/height/pressure
- Cloud top
- Cloud base
- IWP/LWP
- Effective particle size
- Mass-median particle size
- Visible extinction optical thickness
- Infrared emissivity (at 11 μm)

Table 1. List of the cirrus bulk (total-column) properties retrieved by the algorithm outlined in Sections 3 and 4.

Our satellite retrievals have an update frequency of at least 15 minutes – though many of the cases occurred during so-called "super rapid scan" periods where the update frequency can be as short as a few minutes. Using the GOES data, three-dimensional profiles of extinction and effective ice-particle size are generated as follows.

With an estimate in hand for cirrus top and base, along with a parameterization of effective ice-particle size as a function of the cirrus environmental temperature, the cirrus optical thickness at some level z* in the cloud is given by Eq. (23) as

$$\tau_{EXT,VIS} = 3\, IWC(z^*)\, \Delta z / (\rho_{ICE}\, D_{EFF}) , \quad (27)$$

where IWC(z*) is the cirrus layer ice-water content at level z*, Δz is the layer physical thickness (the "IWP" in Eq. (23) equals "IWC(z*) Δz"), and D_{EFF} is the layer's SD effective particle size. It follows that the extinction coefficient $\beta_{EXT,VIS}$ at level z* within

the cirrus is simply

(28) $$\beta_{EXT,VIS}(z^*) = 3\,IWC(z^*) / (\rho_{ICE}\, D_{EFF}) .$$

All that is required to compute Eq. (28) is a satellite-estimated profile of IWC.

Obviously the GOES total-column cirrus radiance observations and IWP retrievals offer little insight as to the nature of the IWC *vertical profile*. However the integrated IWC, or namely the IWP, is a retrievable. To solve the problem of IWC we applied an a-priori knowledge of IWC profile shape using the in-situ radar and lidar observations. We developed a "climatology" of sorts of the radar backscatter and lidar extinction profile shapes using data from the first twenty case-study days. If we assume that the IWC profile shape is the same as the lidar and radar-profile observation average shapes, then the average shape as a function of cirrus physical thickness provides insight into the nature of the IWC profile *shape*. We understand that the correspondence between radar/lidar observation and IWC is not precisely one-to-one. The relation between IWC and attributes like ice-particle size and shape makes the validity of such a direct comparison less tenuous. However, we are pressed with a requirement to generate cirrus extinction coefficient profiles from satellite.

This is the approach we decided to take: with an estimate of cirrus top, base, and an observations-based IWC-profile shape, we assign an absolute IWC(z*) profile (required by Eq. (28)) by constraining the normalized IWC profile to integrate vertically to the retrieved total-column IWP. Figure 3 contains the lidar and radar-based normalized IWC profiles that were observed between cirrus base and top for all observations made during the early portion of the 2005 measurement period, plotted as a function of cirrus physical thickness. Currently we use the 1-to-2.5-km IWC profile shape in our retrievals. Future upgrades will include prescribing IWC shape based on the GOES-retrieved cirrus base and top estimate (i.e., based on the retrieved cirrus physical thickness).

Figure 4 contains a plot of the retrievals for a seven-hour collection period on 29 July 2005. The figure shows direct comparisons between the lidar return, depicted as the color-coded watermark image in the background, and coincident satellite-based retrievals from our cirrus bulk-property retrieval algorithms (see Table 1). Diamonds (squares) denote our cloud-top (base) retrievals, and the red triangles denote the cirrus effective-temperature (radiative "center-of-mass") estimate for the GOES pixel directly over the lidar. Note that the balloon sounding made near the beginning of the observation period and shown on the right of the figure also shows skill at identifying the height of the cirrus base and top (more later). The tabulated values listed below the lidar image are a time series of pixel-level retrievals for the cirrus cloud that was closest to Hanscom for that particular time. Each row is interpreted as follows: **eTIR** is

the 11-μm emissivity times 100 (e.g., 35 means 0.35); **tau** is the 0.55-μm extinction optical thickness times 100 (e.g., 9 means 0.09); **IWP** is the cirrus ice-water path (g/m^2); **Deff** is the ice-particle SD effective size (μm) (again, defined as the ratio of the third to second moment of the ice-particle size distribution); and **T_Cir** is the cirrus effective temperature (K). The effective temperature is the cirrus environmental temperature at the cloud's radiative center of mass and, depending on IWP, usually lies close to the true (i.e., ice) center of mass someplace between cloud base and cloud top.

Note on the right side of Figure 4 that the balloon-observed coincident atmospheric temperature/water-vapor profile does a good job of indicating the presence of cirrus between, say, 9 and 12 km. This type of signature is evident for many (if not most) of the cirrus days at Hanscom, indicating that NWP-based water-vapor profiles might be helpful in assigning and refining cloud top/base estimates *given that the satellite data detect cloud in the first place*. In conditions where clouds are optically thicker, the satellite radiances are minimally influenced by ice particles at the lower portions of the cirrus. Augmenting the weak satellite cloud-base signal with a strong NWP water-vapor-profile signature may prove helpful in apportioning the total retrieved ice mass more accurately between cloud base and cloud top. This influences the magnitude of the retrieved IWC profile and, in turn, the extinction and particle-size profiles.

Figure 5 shows the satellite-based extinction-coefficient profile retrievals (using Eq. (28)) and the coincident lidar and radar observations for the same 29 July case shown above. Note the good agreement between the time dependence of the ground-based observations and the satellite retrievals. Figures 4 and 5 indicate that the satellite retrievals yielded results that are not in conflict with ground-based observation, which in turn helps lend credibility to our GOES-based analyses. Figure 6 contains another sample comparison for 21 June, this time with the 35-GHz radar data. Here we also see good agreement between ground-based observation and satellite retrieval.

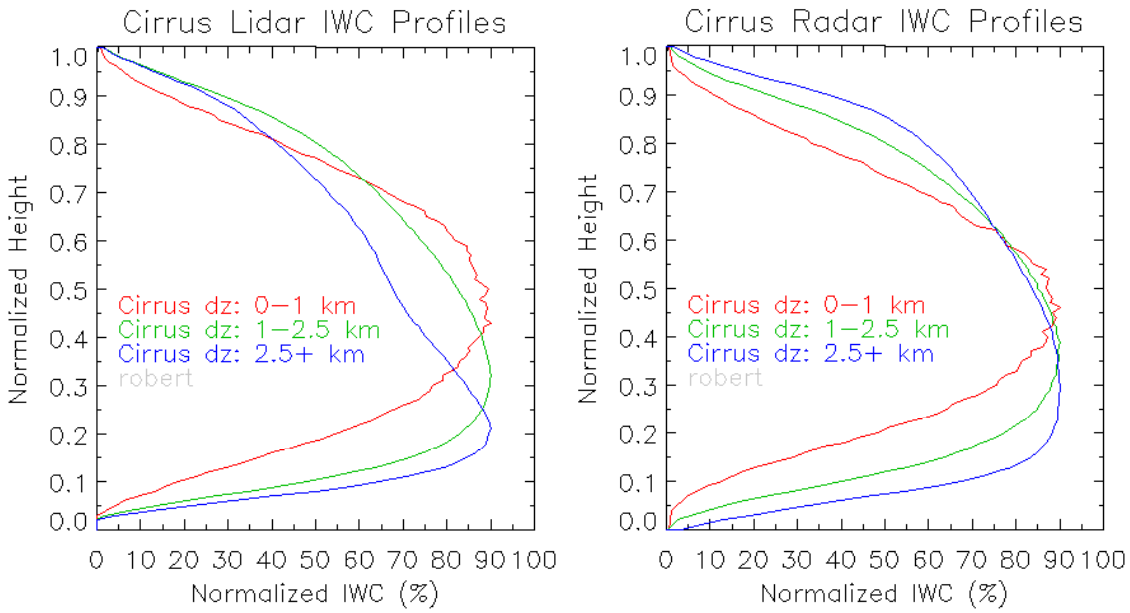

Figure 3. Plots of averaged lidar extinction (left) and radar backscatter (right) observations as a function of normalized in-cloud position for several hundred profiles between February and August 2005. Cloud base is h=0, and cloud top is h=1. These shapes are used to infer the IWC profile shape for any given GOES cirrus pixel

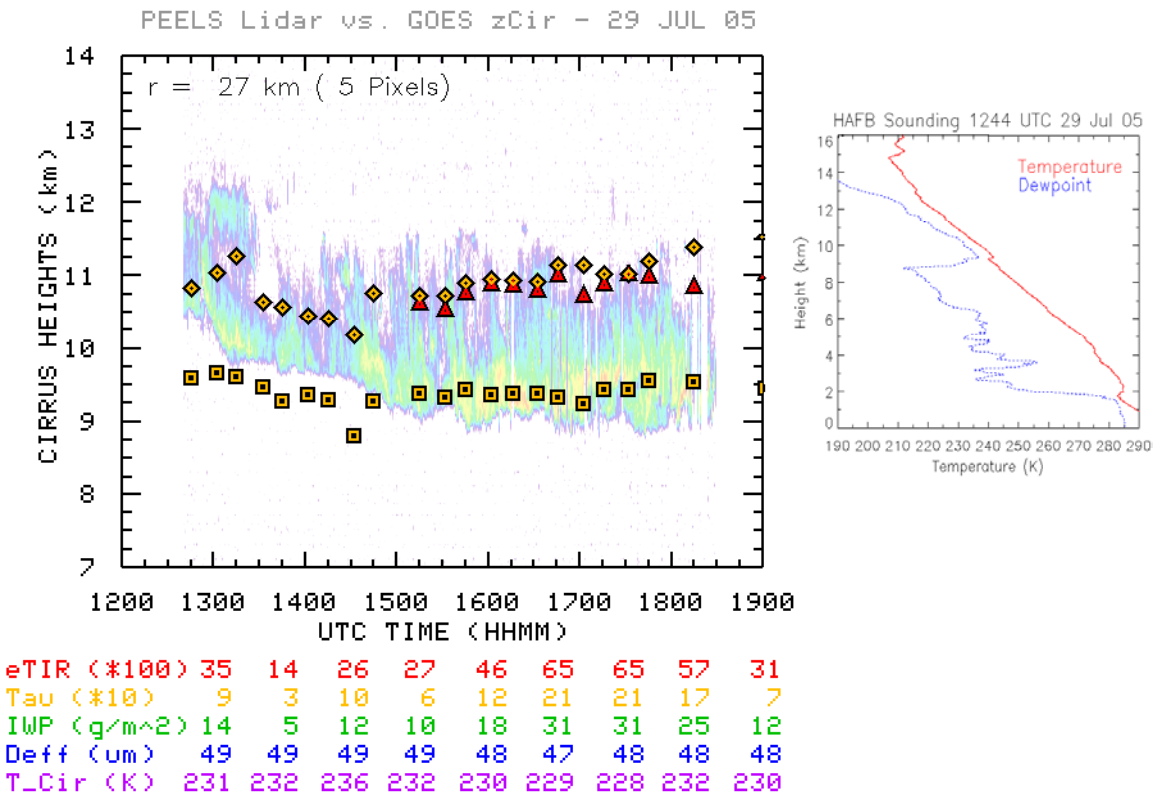

Figure 4. Comparison of GOES cloud-top and base retrievals to PEELS lidar and radiosonde for 29 Jul 05 over Hanscom AFB. Note that the water-vapor sounding does a good job in prescribing the cirrus base and, to a lesser extent, top locations

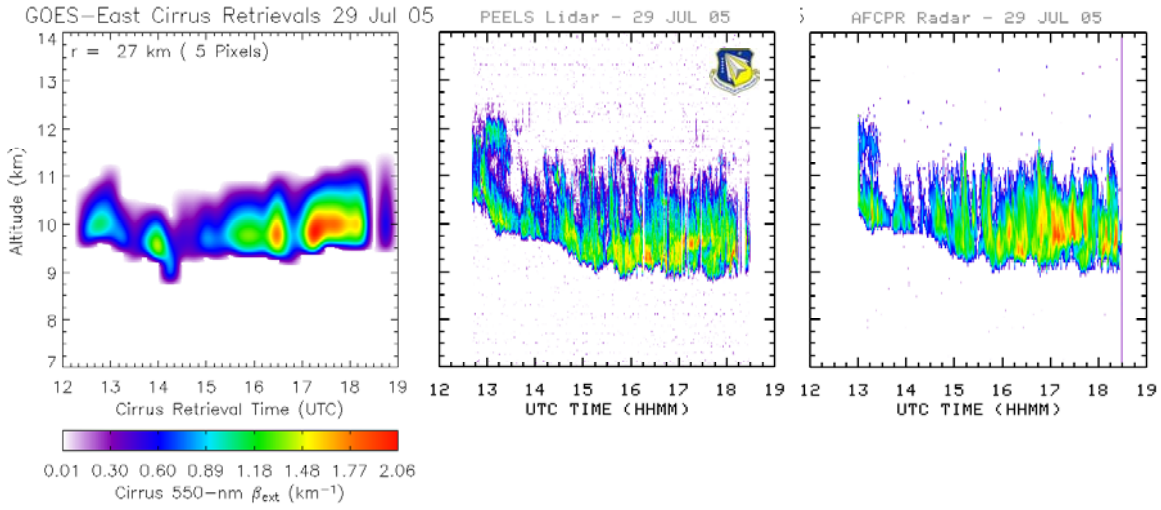

Figure 5. Comparison of satellite-derived extinction profile retrieval (left) to lidar and radar returns for 29 Jul 05 over Hanscom AFB.

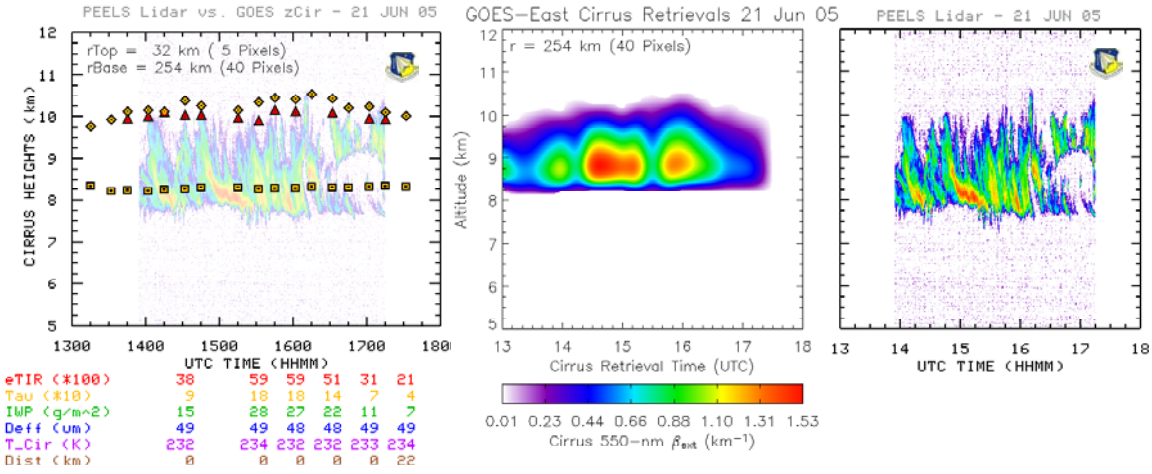

Figure 6. Comparison of satellite derived extinction profile retrieval (left) to lidar returns for 21 June 05 over Hanscom AFB.

5 Summary Remarks

Reasoning behind our approach to IWP and particle-size retrievals is deterministic in nature, whereas our approach to cirrus base and top is empirical. We have repeatedly observed that the local spatial variability in satellite-based cloud effective-height retrievals is observed to be a good predictor of the lidar and radar-observed cloud

vertical bounds. We have found so far that the combined deterministic/empirical technique is observed to perform best for optically thinner cirrus, i.e., for cirrus through which a significant portion of the underlying surface energy is transmitted. Once the cirrus gets optically thick (TIR emissivity > 0.85 or so), cloud bases are typically overestimated because the satellite signal contains little or no information from the deeper parts of the cirrus. Nonetheless we still have a somewhat sensible estimate for cloud base that, in turn, can be used for IWC and extinction computations.

Using this approach we demonstrated our attempts at vertical profiling of extinction coefficients. Figures in Section 4 show two examples of extinction-coefficient vertical profiles retrieved using Eq. (28) along with the normalized IWC shape assumption (see Figure 3) and bulk retrievals in Table 1.

Initial comparisons of the Hanscom AFB lidar and radar data with our bulk satellite retrievals and extinction-coefficient profile estimates are very encouraging. Where these retrievals are of novel use is in their vertical mass-profiling ability. As we learn more about the distribution of ice mass throughout the cirrus depth with these and other data sources (such as those provided more routinely by ARM), we will continue to apply that knowledge to the problem of estimating vertical profiles of ice mass, optical thickness, and particle size for climate radiative forcing and atmospheric heating-rate needs.

6 References

d'Entremont, R. P., and G. B. Gustafson, 2003: Analysis of Geostationary Satellite Imagery Using a Temporal-Differencing Technique. Earth Interactions, **7**, Paper 1.

DeSlover, D., W. L. Smith, P. K. Ppiironen, and E. W. Eloranta, 1999: A methodology for measuring cirrus cloud visible-to-infrared optical depth ratios. Journ. Atmos. Ocean, Tech., **16**, 251-262.

Heymsfield, A. J., and C. M. R. Platt, 1984: A parameterization of the particle size spectrum of ice clouds in terms of the ambient temperature and the ice water content. *Journ. Atmos. Sci.,* **41**, 846-855.

Ivanova, D., D. L. Mitchell, W. P. Arnott, and M. Poellot, 2000: A GCM parameterization of bimodal size spectra and ice-mass removal rates in mid-latitude cirrus clouds. *Atmos. Res.*, **59**, 89-113.

Ivanova, D. C., D. L. Mitchell, and G. M. McFarquhar, 2004: A trimodal size distribution parameterization for tropical cirrus clouds. *Proc. 14th ARM Sci. Team Mtg.*, 22-26 March 2004, Albuquerque.

(www.arm.gov/publications/proceedings/conf14/extended_abs/ivanova-dc.pdf)

Korolev, A., G. A. Isaac, and J. Hallett, 2000: Ice particle habits in stratiform clouds. QJR Meteorol Soc., **126**, 2873-2902.

McFarquhar, G. M., and A. J. Heymsfield, 1997: Parameterization of tropical ice-crystal size distributions and implications for radiative transfer: results from CEPEX. *Journ. Atmos. Sci.*, **54**, 2187-2200.

Mitchell, D. L., R. P. d'Entremont, D. H. DeSlover and W. P. Arnott, 2003: Multispectral thermal retrievals of size distribution shape, effective size, ice water path, optical depth and photon tunneling contribution. *12th Conf. on Satellite Meteorology and Oceanography*, AMS Annual Meeting, Long Beach, California, 9-13 Feb. 2003.

Mitchell, D. L., 2002: Effective diameter in radiation transfer: General definition, applications and limitations. *J. Atmos. Sci.*, **59**, 2330-2346.

Mitchell, D. L., and A. J. Baran, 2002: Testing of the Modified Anomalous diffraction approximation with T-matrix calculations for hexagonal ice columns. *Conf. Atmos. Radiation*, Amer. Meteor. Soc., 3-7 Jun 2002, Ogden UT, J139-144.

Mitchell, D. L., W. P. Arnott, C. Schmitt, A. J. Baran, S. Haveman, and Q. Fu, 2001: Contributions of photon tunneling to extinction in laboratory-grown hexagonal columns. *Journ. Quant. Spectroscopy and Rad. Transf.*, **70**, 761-776.

Mitchell, D. L., D. Ivanova, A. Macke, and G. M. McFarquhar, 2000: A GCM Parameterization of bimodal size spectra for ice clouds. *Proc. 9th ARM Sci. Team Mtg.*, 22-26 March 1999, San Antonio. (www.arm.gov/docs/documents)

Mitchell, D. L., A. Macke, and Y. Liu, 1996: Modeling cirrus clouds. Part II: Treatment of radiative properties. *J Atmos Sci,* **53**, 2967-2988.

Twohy, C. H., A. J. Schanot, and W. A. Cooper, 1997: Measurement of condensed water content in liquid and ice clouds using an airborne counterflow virtual impactor. *J Atmos Ocean Tech*, **14**, 197-202.

Appendix A: Why are SD Shape, Ice Water Path and Effective Size Important?

Satellite-based retrievals of effective diameter (D_{EFF}) and ice water path (IWP) are needed to describe cirrus radiative properties and evaluate their influence on transmittance. Unfortunately these properties are not sufficient for describing the radiative behavior of cirrus at terrestrial wavelengths. Size distribution (SD) shape must also be known for terrestrial radiation. For example, the absorption optical depth may differ up to 44% for two cirrus size distributions having the same D_{EFF} and IWP.

Even knowing the size distribution shape is not totally sufficient for describing the radiative nature of cirrus clouds at infrared wavelengths. This is because a process called photon tunneling often contributes significantly (between 15 and 42%) to the absorption of infrared energy by cirrus ice particles, as shown in Figure A1 below. Tunneling here labels the process by which photons beyond the particle's geometric cross-section are absorbed, in comparison to absorption due strictly to the particle's geometric cross section or internal reflection/refraction. These three processes are illustrated in Figure A2. Contributions to tunneling are greatest when particle size and wavelength are comparable.

Tunneling has been parameterized for ice clouds by Mitchell and Baran (2002), whose radiation scheme was found to be accurate within 15% relative to T-matrix calculations of absorption efficiency (5% mean error) over the wavelength range 2-18 μm (see Figure A1). Additionally, mean extinction efficiency (Q_{EXT}) errors for a hexagonal-column ice cloud were ≤3% relative to measured Q_{EXT} over the same wavelength range (Mitchell, 2001). Hence it appears justifiable to use this radiation scheme, making it necessary to know the tunneling factor t_f, which ranges between 1 (for ice spheres) and 0 (no tunneling).

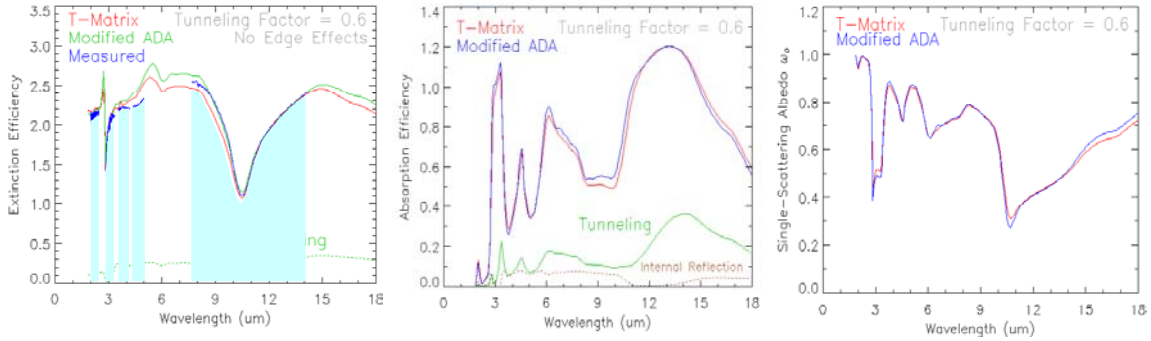

Figure A1. Plots of MADA extinction and absorption efficiencies, and single-scattering albedo, for an observed distribution of cirrus ice particles. Also plotted for comparison are T-matrix theory computations for the same SD. (See Mitchell, 2002)

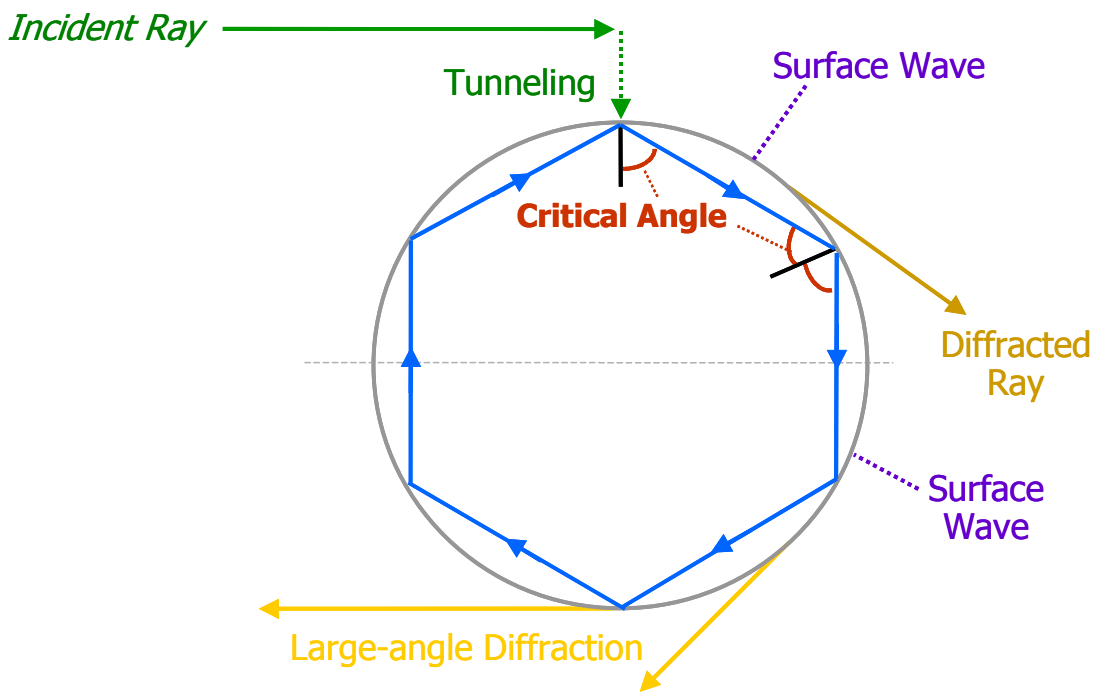

Figure A2. Depiction of the possible trajectories of an incident ray grazing a cloud particle. Photons beyond the physical cross section undergo "tunneling" into the edge domain, launching surface waves that are continually dampened as they propagate.

Appendix B: Improving Particle-Size Retrievals

As mentioned in Section 3.2.6, we have exploited a means of estimating the ice-particle effective size D_{EFF} as a function of cirrus environmental temperature. Although this assumption bears out in a time- and space-average sense, we acknowledge its shortcomings on a pixel-by-pixel basis. From the climate-forcing point of view, longwave infrared fluxes are dominated by cloud absorption optical thickness profiles. To the extent that absorption optical thickness depends on effective particle size, more accurate estimates of D_{EFF} may be required.

However, note from Eq. (20) that the direct influence of D_{EFF} on τ_{ABS} is moderated by the absorption efficiency Q_{ABS}; in other words, for infrared absorption and emission properties, absorption optical thickness is linear with IWP and the *ratio* Q_{ABS}/ D_{EFF} of absorption efficiency to effective particle size. Thus as long as the relationship between Q_{ABS} and D_{EFF} is radiatively consistent, then our retrievals of cirrus absorption properties is likely not to be suffering too much from a perhaps oversimplified parameterization between D_{EFF} and T_{CI}.

Where all of this falls apart, of course, is when scattering plays an important role in the radiation transfer. Although its influence on infrared radiances is relatively weak, scattering plays a dominant and forceful role in the scattering of sunlight at visible, near-IR, and SWIR wavelengths. This is when a more deterministic approach to retrieving D_{EFF}, and its relation with asymmetry and single-scattering albedo, is called for. To this end, we plan to incorporate the following retrieval scheme for effective particle size.

Cirrus emissivities, and hence τ_{ABS}, can be obtained spectrally from the available infrared channels of a satellite imager. In combination with a spectrum of retrieved absorption optical thicknesses, the modified anomalous diffraction theory we use for computing scattering and absorption efficiencies can be exploited to retrieve particle size. In Figure B1 it can be seen that ratios of absorption optical thickness at a given wavelength to that at 11 μm contains useful information on the effective particle size of our bimodal size distributions. From Eq. (20) it is seen that this ratio is simply the ratio $Q_{ABS}(\lambda)/ Q_{ABS}(11\ \mu m)$ since particle size and IWP are wavelength-invariant properties. This technique is similar to that outlined by DeSlover et al (1999).

The plots in Figure B1 were obtained using our MADA absorption efficiency theory outlined in Section 3.2.2, along with the bimodal mid-latitude and tropical cirrus size-distribution aircraft observations. Note hat there is a strong dependence of this ratio on particle size for most of the infrared bands available on operational meteorological satellites, including the WV and TIR bands.

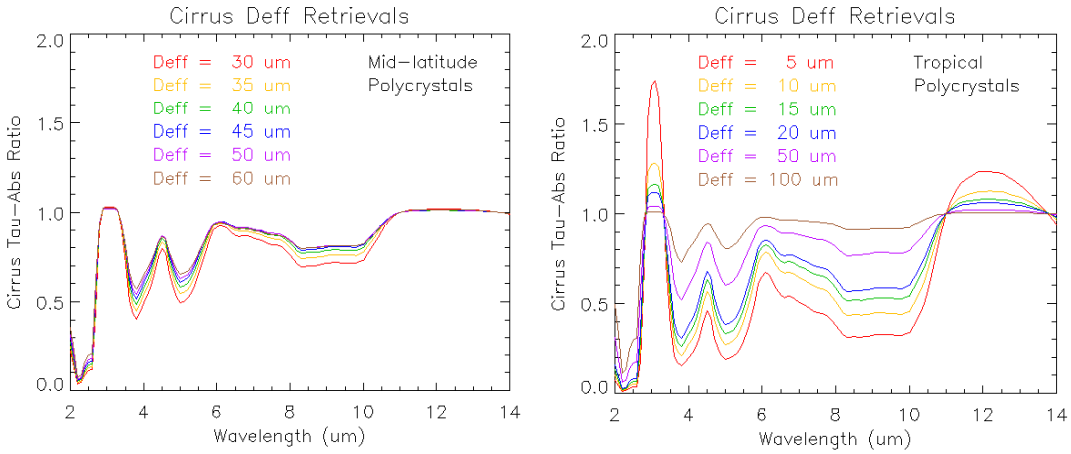

Figure B1. Plots of the absorption efficiency ratios predicted by our MADA theory as a function of effective particle size, for mid-latitude (left) and tropical (right) bimodal distributions of cirrus ice particles.

The plots show that by ratioing satellite-retrieved absorption optical thickness combinations of 3.9/11 μm or 8.55/11 μm, it is possible to retrieve D_{EFF}. These curves were generated using the ice-cloud radiation model described in Mitchell (2002), assuming N(D) for both tropical and mid-latitude cirrus, and for shapes that include rosettes, plates, hexagonal columns, and planar polycrystals. Mitchell (2002) describes that size distributions with differing D_{EFF} values can have the same radiative properties because of the behavior of the small- and large-particle modes. These curves provide insight to expected retrieval accuracies of D_{EFF}, as well as the influence of bimodal particle distributions on absorption. Size information is best obtained when using infrared bands where absorption is volume- (mass) dependent, such as at 3.9 μm. At 10.1 μm, absorption is partially mass and partially area-dependent, but is strongly area-dependent at 11.2 μm.